

# Investigation of the Selective Production of Ethylene from Propylene Over Small-Pore Zeolites

Jong-Won Jun<sup>1</sup>, Tae-Wan Kim<sup>1,2,\*</sup>, and Chul-Ung Kim<sup>1,2</sup>

<sup>1</sup>Center for Convergent Chemical Process, Korea Research Institute of Chemical Technology,  
141 Gyeong-ro, Yuseong, Daejeon 34114, Republic of Korea

<sup>2</sup>Department of Advanced Materials and Chemical Engineering, University of Science and Technology (UST),  
217 Gajeong-Ro, Daejeon 34114, Yuseong, Republic of Korea

The selective production of ethylene from the direct conversion of propylene (propylene-to-ethylene, PTE) was examined for the first time using various types of 8-membered ring (8-MR) zeolite materials with different pore structures. Among these 8-MR zeolites, SSZ-13 zeolite with a three-dimensional chabazite structure exhibited the highest ethylene yield. To increase the ethylene selectivity further, the PTE reactions were conducted over SSZ-13 zeolite external surface modifications with silylation or phosphorus. The external surface modifications enhanced the ethylene selectivity due to the passivation of external acid sites. The surface-modified SSZ-13 catalyst exhibited the highest selectivity to ethylene, at more than 90% at 450 °C, a WHSV of 0.33 h<sup>-1</sup>, and a propylene particle pressure of 0.1 MPa.

**Keywords:** Propylene-to-Ethylene, Olefin Interconversion, Surface-Modified SSZ-13.

## 1. INTRODUCTION

Zeolites are particularly useful catalysts in industrial applications. Microcellular networks of zeolite materials provide unique shape selectivity. In particular CHA (chabazite) zeolites with 3-dimensionally 8-membered ring (8-MR) have been used to produce light olefins from methanol.<sup>1</sup> Light olefins such as ethylene and propylene are the major bulk chemicals currently produced by the petrochemical industry.<sup>2</sup> These light olefins are used as major petrochemical building blocks for the manufacturing of various industrial products, such as packaging, rubber, construction, textiles and furniture, as well as plastic products. Propylene is a very important raw material for polypropylene, propylene oxide, and acrylonitrile, and is usually produced by means of the naphtha cracking process. However, the supply of ethylene may be deficient (compared with the amounts needed) in the near future owing to the rapid increase in the supply of ethylene from ethane crackers and shale gas. Therefore, the co-production of ethylene and propylene through the PTE process as a post-process using the above ethylene has attracted much attention recently.<sup>1</sup> In recent years, chabazite zeolites such as SAPO-34 and SSZ-13 have been reported in relation to the selective production

of propylene from ethylene. The selective production of propylene to ethylene was initially explored with various types of zeolites in a continuous fixed-bed reactor. ZSM-5 has stable and low selectivity. However, small-pore zeolite shows high selectivity to ethylene.<sup>3</sup> Therefore, a PTE reaction was carried out using various types of 8-MR zeolite. The CHA-based SSZ-13 zeolite was studied with regard to the effect of ethylene selectivity on the PTE reaction. SSZ-13 zeolite surface modifications of silylation and phosphorus have also been systematically studied to ascertain the relationship between the PTE results and the characteristics of the zeolite.

## 2. EXPERIMENTAL DETAILS

### 2.1. Preparation of the Catalysts

SSZ-13 was purchased from China Catal. Holding Co. and SAPO-34, SAPO-17, SAPO-18, and Rho zeolite were prepared in our laboratory.<sup>4-5</sup> An outer-surface passivating modification of the SSZ-13-T(X) (X refers to the TEOS silylation time) catalyst was carried out using TEOS (Si(OCH<sub>2</sub>CH<sub>3</sub>)<sub>4</sub>, Aldrich, 99%) silylation.<sup>6</sup> The phosphorous-modified SSZ-13 samples were prepared by the simple impregnation of phosphoric acid in an ethanol and water mixture.<sup>3</sup> This is referred to here as SSZ-13-P(Y) (with Y denoting the P loading amount).

\*Author to whom correspondence should be addressed.

## 2.2. Characterization

Powder X-ray diffraction (XRD) patterns were recorded on a Rigaku Multiplex instrument using Cu-K $\alpha$  radiation ( $\lambda = 0.15406$  nm) operated at 40 kV and 40 mA (1.6 kW). Nitrogen physisorption isotherms were measured at  $-196$  °C on a Micromeritics ASAP 2020 instrument. The Si/Al<sub>2</sub> ratios and *P* loading amounts were determined by inductively coupled plasma-atomic emission spectroscopy (ICP-AES) using an Optima 4300 DV instrument (Perkin Elmer). Acid sites were measured by the temperature-programmed desorption of ammonia (NH<sub>3</sub>-TPD) using a BELCAT-M (BEL Japan) instrument. The degree of coke deposition of the catalyst was investigated by recording weight changes on a thermogravimetric analyzer (DTG-60, Shimadzu).

## 2.3. Catalytic Test

The propylene-to-ethylene (PTE) reaction was conducted in a lab-made fixed-bed reactor system. Pretreatment with 0.5 g of the catalyst was carried out at 550 °C under an N<sub>2</sub> flow for 3 h (50 ml/min). The typical PTE reaction was performed at a weight hourly space velocity (WHSV) of 0.33 h<sup>-1</sup> at 450 °C under ambient pressure. The effluent products were analyzed by an online gas chromatograph (6100GC, Young Lin Instruments, Co.). The conversion of propylene was calculated from the GC-TCD signal of nitrogen and propylene using an alumina column (50 m  $\times$  0.53 mm I.D.). The light hydrocarbon (carbon number = C<sub>1</sub>–C<sub>4</sub>) and heavy hydrocarbon (C<sub>5+</sub>) products generated from the reaction were analyzed by two GC-FID signals, one from an alumina column (50 m  $\times$  0.53 mm I.D.) and the other from a DHA column (100 m  $\times$  0.25 mm I.D.).

## 3. RESULTS AND DISCUSSION

### 3.1. Effects of the Zeolite Pore Structure on the PTE Activity

Five zeolite materials in total were prepared to evaluate the effects of the zeolite pore structure on the PTE. As shown in Table I, these zeolites are classified according to their topologies. All of the 8-MR zeolite materials exhibited distinct XRD peaks with high signal intensities (Fig. 1),

**Table I.** Physicochemical properties of the 8-MR zeolites with various structures.

Zeolites	Topology	Si/Al <sub>2</sub> <sup>a</sup>	S <sub>BET</sub> <sup>b</sup> (m <sup>2</sup> g <sup>-1</sup> )	V <sub>tot</sub> <sup>c</sup> (cm <sup>3</sup> g <sup>-1</sup> )	TA <sup>d</sup> (mmol g <sup>-1</sup> )
SAPO-17	ERI	0.03	480	0.19	0.42
SAPO-18	AEI	0.21	532	0.22	0.37
SAPO-34	CHA	0.32	456	0.42	1.32
SSZ-13	CHA	27.8	668	0.64	0.95
Rho	RHO	4.51	552	0.26	0.55

Notes: <sup>a</sup>Si/Al<sub>2</sub> molar ratio obtained from ICP-AES elemental analysis. <sup>b</sup>S<sub>BET</sub> is the BET surface area obtained from N<sub>2</sub> adsorption in a relative pressure range (*P*/*P*<sub>0</sub>) of 0.05–0.20. <sup>c</sup>V<sub>tot</sub> is the total pore volume obtained at *P*/*P*<sub>0</sub> = 0.95. <sup>d</sup>TA is the total acidity obtained from the NH<sub>3</sub>-TPD analysis.

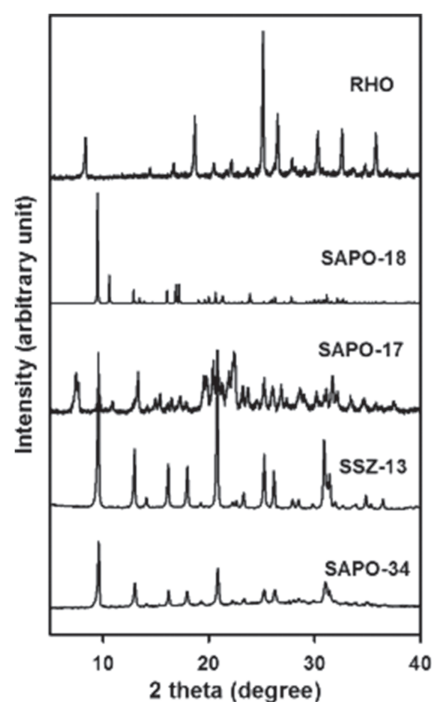


**Figure 1.** Powder XRD patterns of the 8-MR zeolites with various structures.

and their XRD patterns were found to be identical to the desired zeolitic structures in a comparison with reference XRD patterns in the IZA database. The specific BET surface areas and total pore volumes of the zeolite materials with different structures were determined by a nitrogen physisorption analysis (Table I).

The zeolite materials with various structures underwent PTE reactions as catalysts at a fixed reaction condition of 450 °C with a WHSV of 0.33 h<sup>-1</sup>. As shown in Figure 2, the 8-MR zeolite with the 3-D CHA structure, Rho, shows the steepest decrease in the propylene conversion during the initial reaction period (<2 h). Compared with SAPO-34, SSZ-13 has a high ethylene yield and high ethylene selectivity (Figs. 2(b and c)). The 8-MR zeolite showed relatively gradual deactivation of the catalyst from low C<sub>3=</sub> conversion in the initial reaction period, and the propylene conversion reached a plateau (~20%) after 7.5 h. However, the ethylene selectivities of these 8-MR zeolites exceeded 20% for the entire reaction time (Fig. 2). From these PTE results of the 8-MR zeolites, the mass transfer of the reactants and products may not arise, and the pores may be blocked more easily by the formation of coke due to the smaller pore channels (cage windows).

### 3.2. Effects of a Zeolite Surface Modification on the PTE Activity

For the further improvement of the PTE activity, the SSZ-13 zeolite was selected due to a relatively high ethylene yield compared to the other 8-MR zeolites. Especially, to obtain the high ethylene selectivity, we applied the

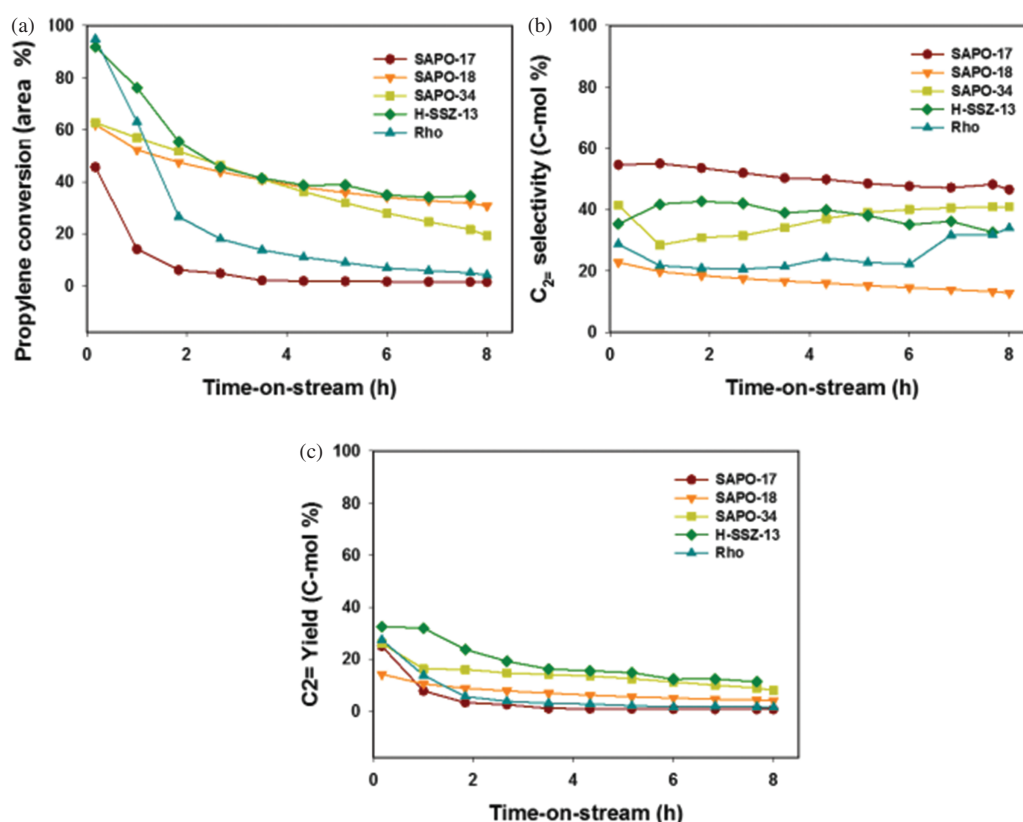


**Figure 2.** Propylene conversion (a), ethylene selectivity (b), and (c) ethylene yield of the 8-MR zeolites with the time-on-stream.

passivation of external surface acid sites to the SSZ-13 zeolite using treatments of phosphorous and TEOS, which are typically used to remove acid sites of the outer surface of small pore zeolites.

The Si/Al<sub>2</sub> ratios increased significantly after both modifications. Furthermore, from the variation of the BET surface areas of the TEOS and P modified catalysts, as shown in Table II, it was found that the total surface area of the parent TEOS and the P-modified catalyst decreased sharply from 668 m<sup>2</sup>/g to 613–633 m<sup>2</sup>/g after the modification. From the results shown in Figure 3, it was confirmed that a decrease in the number of strong acid sites occurred

in the two treated catalysts compared to the commercial H-SSZ-13. These samples also exhibit a lower desorption temperature at the strong acid sites, indicating the weakened strengths of the acid sites after the TEOS and P treatment. In particular, the significant decrease in the number of strong acid sites on the catalyst during the TEOS and P treatment can be attributed to a decrease in the framework Al. The TEOS and P treatment is an effective means of decreasing the acid amount and acid strength.<sup>7</sup>

**Table II.** Physicochemical properties of surface-modified SSZ-13 zeolites with silylation and phosphorus.

Catalysts	<i>p</i> <sup>a</sup> (wt%)	Si/Al <sub>2</sub> <sup>b</sup>	<i>S</i> <sub>BET</sub> <sup>c</sup> (m <sup>2</sup> g <sup>-1</sup> )	Acid concentration (mmol/g) <sup>d</sup>		Total acid site
				Weak	Strong	
H-SSZ-13	–	27.8	668	0.055	1.261	1.32
SSZ-13-T1	–	35.4	625	0.058	0.849	0.91
SSZ-13-T2	–	35.9	633	0.056	0.784	0.85
SSZ-13-P0.25	0.24	35.2	613	0.564	0.816	1.38
SSZ-13-P0.5	0.52	36.4	618	0.412	0.798	1.21

Notes: <sup>a</sup>, <sup>b</sup> Si/Al<sub>2</sub> molar ratio obtained from the ICP-AES elemental analysis. <sup>c</sup> *S*<sub>BET</sub> is the BET surface area obtained from N<sub>2</sub> adsorption in a relative pressure range (*P*/*P*<sub>0</sub>) of 0.05–0.20. <sup>d</sup> Acid concentration obtained from the NH<sub>3</sub>-TPD analysis.

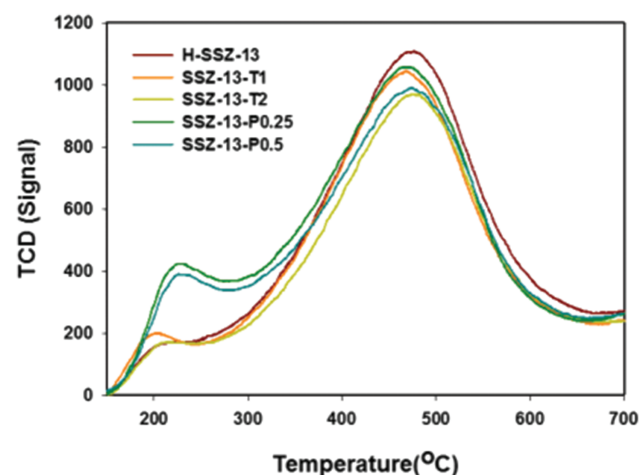


**Figure 3.** NH<sub>3</sub>-TPD pattern of the modified SSZ-13s.

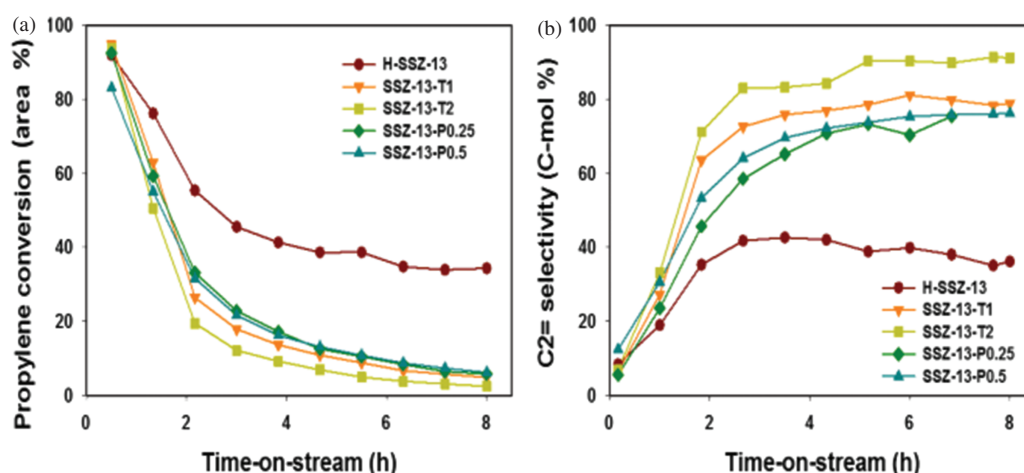


**Figure 4.** Propylene conversion (a) and ethylene selectivity (b) of surface-modified SSZ-13 zeolites during the time-on-stream.

In order to investigate the effect of the surface modification, PTE reactions of the 0.25% and 0.5% P-SSZ-13 catalysts were carried out, as described below. As the content of P increased, the deactivation occurred more rapidly at the initial stage of the reaction and at the point of the maximum ethylene yield. Figure 4 shows the propylene conversion and ethylene selectivity in the PTE reaction as a function of time using the surface-modified SSZ-13 zeolites with TEOS and P. The modified SSZ-13 zeolites

exhibited lower propylene conversion and higher ethylene selectivity than the original SSZ-13 over the entire reaction time. Among these samples, the SSZ-13-T2 showed the highest ethylene selectivity up to 90%.

As a result, the external surface passivation of SSZ-13 zeolites resulted in an enhanced selectivity towards ethylene in the PTE reaction. In addition, an optimal passivation treatment could be set for each SSZ-13s zeolite under investigation.

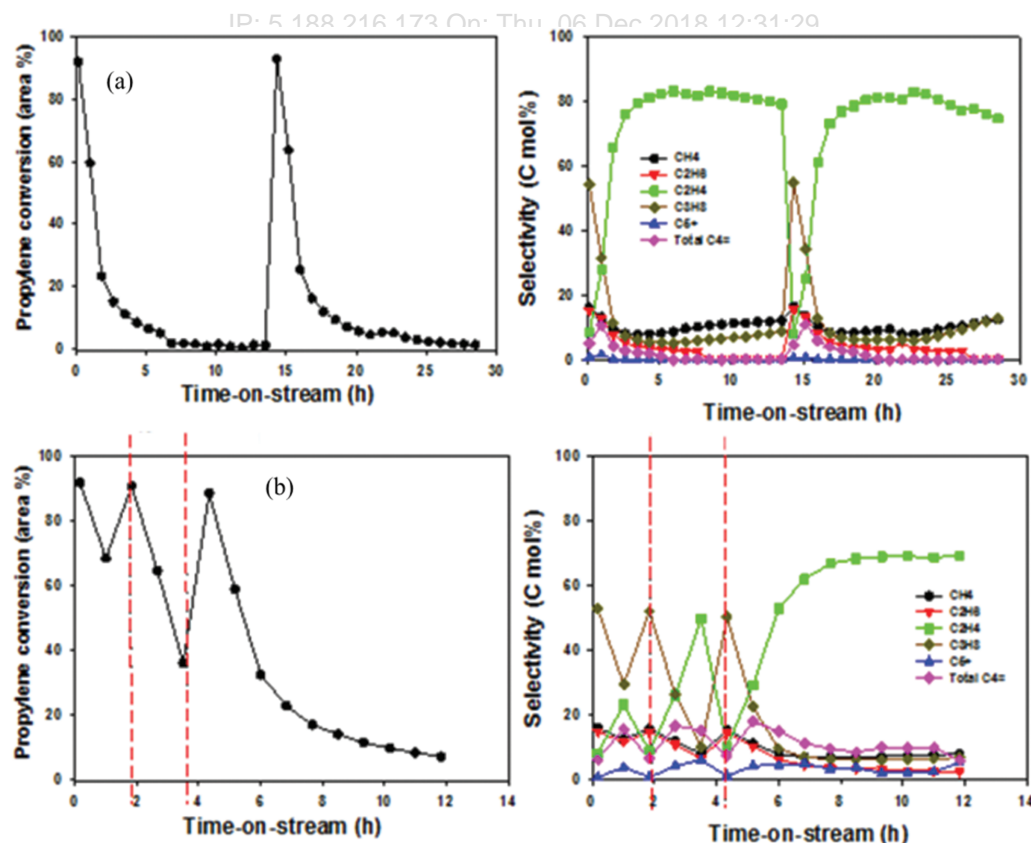


**Figure 5.** Propylene conversion and product selectivities of the SSZ-13-T2 catalyst during the time-on-stream in the regeneration test with air: Regeneration of (a) fully deactivated and (b) partially deactivated spent samples.

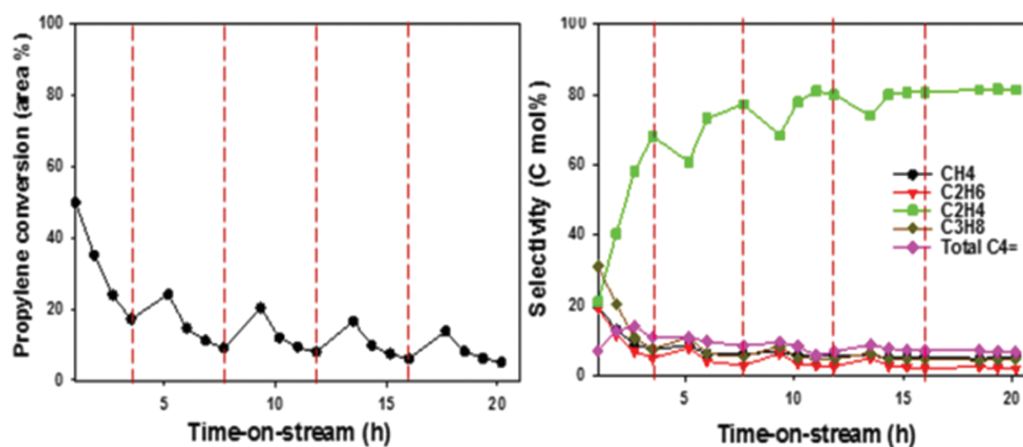


**Figure 6.** Propylene conversion and product selectivities of the SSZ-13-T2 catalyst during the time-on-stream in the regeneration test with hydrogen.

### 3.3. Regeneration Test

As shown in Figure 5(a) the fully deactivated catalyst was completely regenerated by the removal of coke from the cages of the SSZ-13 zeolite. The coke in the zeolite cages were burnt under an air flow 550 °C. After

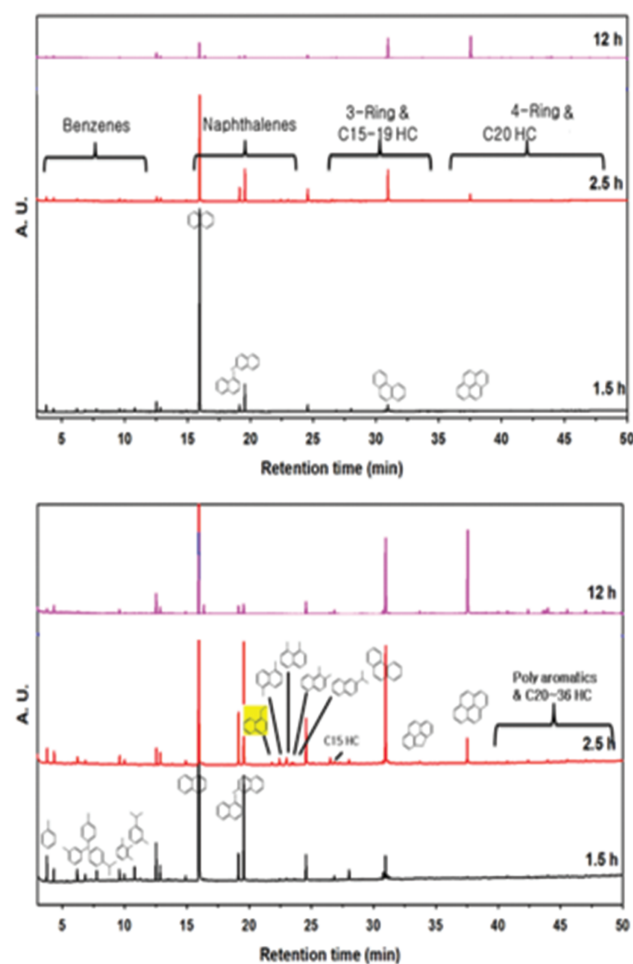


**Figure 7.** GC-MS chromatograms (top) and magnified chromatograms (down) of the extracts from the spent SSZ-13 catalysts.

regeneration of the partially deactivated catalyst by air (dotted red-line), the propane selectivity was always higher than ethylene selectivity at the initial reaction period (Fig. 5(b)). Figure 6 shows the regeneration of partially deactivated SSZ-13-T2 catalysts using a hydrogen flow at 500 °C. The H<sub>2</sub> regeneration exhibited stable ethylene selectivity of around 75~80% throughout the reaction time. This occurs because the H<sub>2</sub> partially removed the coke from the cage of the SSZ-13 zeolite. Moreover, there was no initial induction period after the H<sub>2</sub> regeneration process.

For the study of reaction mechanism, three extracted coke samples from the spent catalysts with different reaction times (1.5, 2.5 and 12 h) were prepared for the GC-MS analysis. As shown in Figure 7, naphthalene is the main product at the beginning of the reaction (1.5 h); however naphthalene derivatives and phenanthrene are produced at the reaction time of 2.5 h. Among the various naphthalene derivatives produced in this stage, ethyl naphthalene would be a main precursor to produce ethylene via bond cleavage reaction inside cages of the SSZ-13. These coke analysis results are similar to these of the spent SSZ-13 catalyst in the ethylene-to-propylene (ETP) reaction.<sup>8</sup> In the proposed reaction mechanism of ETP reaction, ethylene is rapidly oligomerized and converted to naphthalene-based intermediates in the cage of SSZ-13. Among these reaction intermediates, propyl naphthalene would be the main intermediate to selectively produce propylene via bond cleavage between naphthalene and propyl-group. In addition, poly-aromatic and heavier fractions were also formed as the reaction times become longer. It is due to that these large amount of organic intermediates and coke formed inside the CHA cages, and deactivated the catalyst rapidly.

## 4. CONCLUSION

SSZ-13 showed the highest ethylene yield among the 8-MR zeolites in the PTE reaction. Further surface modification with TEOS or P enhanced the ethylene selectivity

up to 90% due to the passivation of external acid sites. Hydrogen regeneration was essential to maintain high ethylene selectivity without initial induction period. The analysis of the coke extraction might show the formation of the ethyl naphthalene intermediate in the SSZ-13 cages, which was converted to ethylene in the cage of SSZ-13 selectively.

**Acknowledgment:** This work was supported by the National Research Council of Science and Technology (NST) grant by the Korea government (Ministry of Science and ICT (MSIT)) (No. CRC-14-1-KRICT).

## References and Notes

1. J. W. Jun, N. A. Khan, P. W. Seo, C. U. Kim, H. J. Kim, and S. H. Jung, *Chem. Eng. J.* 303, 667 (2016).
2. S. M. Sadrameli, *Fuel* 173, 285 (2016).
3. J. W. Jun, T. W. Kim, S. I. Hong, J. W. Kim, S. H. Jung, and C. U. Kim, *Catal. Today* <http://doi.org/10.1016/j.cattod.2017.10.004>.
4. Y. Ji, J. Birmingham, M. A. Deimund, S. K. Brand, and M. E. Davis, *Micro. Meso. Mater. MM* 232, 126 (2016).
5. US patent 4,440,871.
6. P. Losch, M. Boltz, C. Bernardon, B. Louis, A. Palčić, and V. Valtchev, *Appl. Catal. A: Gen.* 509, 30 (2016).
7. C. Zhang, X. Guo, C. Song, S. Zhao, and X. Wang, *Catal. Today* 149, 196 (2010).
8. W. Dai, X. Sun, B. Tang, G. Wu, L. Li, N. Guan, and M. Hunger, *J. Catal.* 314, 10 (2014).

Received: 15 January 2018. Accepted: 13 February 2018.

IP: 5.188.216.173 On: Thu, 06 Dec 2018 12:31:29  
Copyright: American Scientific Publishers  
Delivered by Ingenta